AIP Applied Physics Letters

Atomic layer deposition of ZrO 2 on W for metal–insulator–metal capacitor application

Sang-Yun Lee, Hyoungsub Kim, Paul C. McIntyre, Krishna C. Saraswat, and Jeong-Soo Byun

Citation: Applied Physics Letters **82**, 2874 (2003); doi: 10.1063/1.1569985
View online: http://dx.doi.org/10.1063/1.1569985
View Table of Contents: http://scitation.aip.org/content/aip/journal/apl/82/17?ver=pdfcov
Published by the AIP Publishing

Atomic layer deposition of ZrO_2 on W for metal–insulator–metal capacitor application

Sang-Yun Lee, Hyoungsub Kim,[a] and Paul C. McIntyre
Department of Materials Science and Engineering, Stanford University, Stanford, California 94305

Krishna C. Saraswat
Department of Electrical Engineering, Stanford University, Stanford, California 94305

Jeong-Soo Byun
Applied Materials, Inc., 3330 Scott Boulevard, Santa Clara, California 95054

(Received 6 January 2003; accepted 1 March 2003)

A metal–insulator–metal (MIM) capacitor using ZrO_2 on tungsten (W) metal bottom electrode was demonstrated and characterized in this letter. Both ZrO_2 and W metal were synthesized by an atomic layer deposition (ALD) method. High-quality 110∼115 Å ZrO_2 films were grown uniformly on ALD W using $ZrCl_4$ and H_2O precursors at 300 °C, and polycrystalline ZrO_2 in the ALD regime could be obtained. A 13∼14-Å-thick interfacial layer between ZrO_2 and W was observed after fabrication, and it was identified as WO_x through angle-resolved x-ray photoelectron spectroscopy analysis with wet chemical etching. The apparent equivalent oxide thickness was 20∼21 Å. An effective dielectric constant of 22∼25 including an interfacial WO_x layer was obtained by measuring capacitance and thickness of MIM capacitors with Pt top electrodes. High capacitance per area (16∼17 fF/μm^2) and low leakage current (10^{-7} A/cm^2 at ±1 V) were achieved. © *2003 American Institute of Physics.* [DOI: 10.1063/1.1569985]

With the continuing down-scaling of integrated circuit dimensions, high-density dynamic random access memory (DRAM) requires increasing capacitance per unit area to improve sensing and noise immunity.[1] Several possible high-*k* materials, such as Al_2O_3 ($\varepsilon_r=10$),[2] Ta_2O_5 ($\varepsilon_r=26$),[3] and (BaSr)TiO_3 (BST) ($\varepsilon_r=200\sim350$)[4] have been investigated to meet the required trend of relentless device miniaturization. However, Ta_2O_5 and BST are usually thermodynamically unstable with the bottom electrode used in such capacitors (in particular, with doped poly-Si), and, as a result, it is difficult to control the stoichiometry of films during the subsequent thermal treatment.[3,4] Al_2O_3 is stable in contact with many bottom electrodes; however, it has a rather low dielectric constant which limits its effectiveness as an enabler for continued on-chip capacitor dimensional scaling. Recently, ultrathin films of other high-*k* dielectric materials, such as ZrO_2 and HfO_2 have been are widely studied, especially for gate dielectric applications, because of their relatively high dielectric constant (∼25) and thermodynamic stability.[5] However, little is known regarding the behavior of these metal-oxide films in metal–insulator–metal (MIM) structures for charge storage capacitor applications in DRAM devices.

Among the possible deposition techniques for preparing nanoscale high-*k* dielectric films, atomic layer deposition (ALD) is very promising, because it can produce high quality films with precise thickness control and near-perfect conformality, which are crucial for nonplanar structures, such as three-dimensional high-geometry capacitors. The conformality of ALD film growth results from its adsorption-controlled deposition mechanism.[6] As a consequence, high-*k* metal-oxide films, such as ZrO_2 synthesized by ALD,[7] could be strong candidates for capacitor dielectric materials in high density DRAMs requiring complicated capacitor geometries.

In terms of the bottom electrode, highly doped poly-Si is conventionally used in DRAM capacitors. However, it easily reacts with high-*k* dielectric materials and generates thick interfacial oxides having a low dielectric constant.[8] Therefore, MIM capacitors using transition metals, such as Pt, Ru, Ta, and W, as bottom electrodes, have been considered for future capacitor structures.[9] Recently, ALD deposition of a single-element metal like W using WF_6 and Si_2H_6 was demonstrated for filling contacts and vias in microelectronic circuits.[10]

In this letter, results are reported on the preparation and properties of a high-quality thin ALD-ZrO_2 dielectric layer which was deposited on an ALD-W metal electrode to form a MIM capacitor structure with a Pt top electrode. The compositional and structural properties were investigated using transmission electron microscopy (TEM) and angle-resolved x-ray photoelectron spectroscopy (ARXPS). Electrical properties, such as capacitance–voltage and leakage-current–voltage characteristics, were measured using MIM capacitors.

An ALD-W film of 500-Å thickness was deposited at 300 °C on a TiN/SiO_2/Si structure using tungsten hexafluoride (WF_6) and diborane (B_2H_6) as the precursors. Without any surface pre-cleaning of the W, 110∼115 Å of ZrO_2 was deposited at 300 °C using alternating surface-saturating reactions of $ZrCl_4$ and H_2O in a cold wall-type, high-vacuum laboratory-scale ALD system. Each precursor was pulsed for 2 s and N_2 purging followed for 30 or 60 s after H_2O or $ZrCl_4$ pulsing, respectively. The base pressure of the system was in the mid-10^{-8} Torr range and the process pressure was maintained at 0.5 Torr. Various process results, such as a deposited thickness that depends linearly on the number of $H_2O/ZrCl_4$ cycles, the independence of growth rate on pre-

[a]Author to whom correspondence should be addressed; electronic mail: hsubkim@stanford.edu

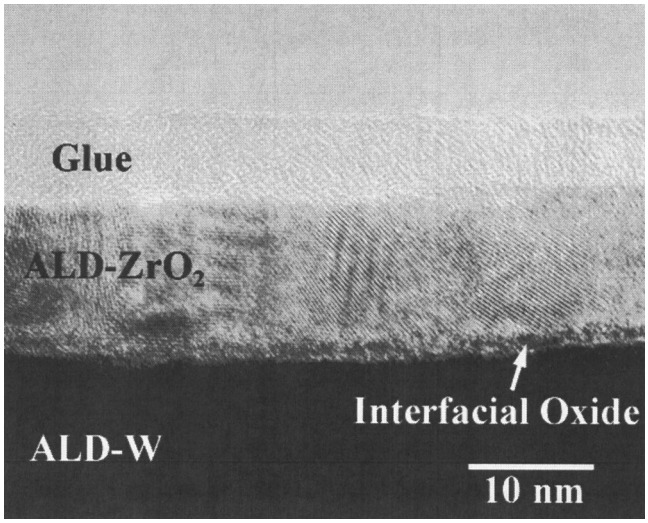

FIG. 1. Cross-sectional HR-TEM micrograph of ALD-ZrO_2/ALD-W.

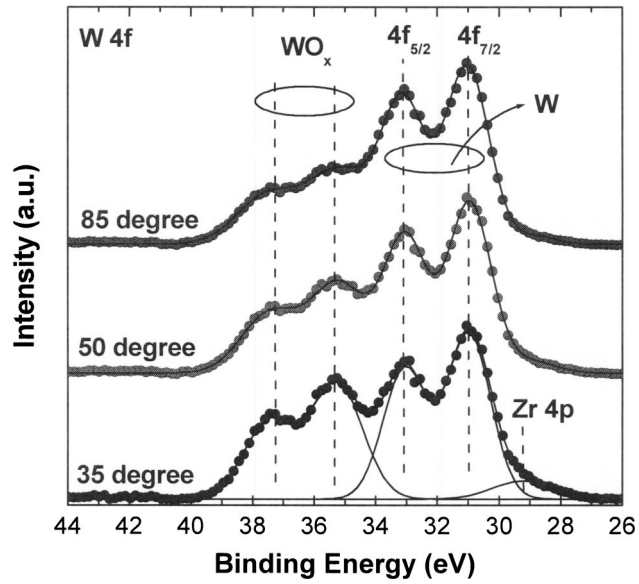

FIG. 2. X-ray photoelectron spectrum of W $4f$ on ALD-ZrO_2/ALD-W specimen after HF etching of the ZrO_2 layer as a function of the detection take-off angle.

cursor pulse and purging duration, and the near-perfect step coverage on a high-aspect-ratio structure, confirmed that the ZrO_2 process used in this experiment was in the ALD regime. No annealing experiments to densify the ZrO_2 film were performed after capacitor fabrication.

In order to measure the electrical properties of the MIM capacitors, various sizes of circular Pt electrodes were deposited by e-beam evaporation through a shadow mask. The compositional characterization and the depth profiling of a ZrO_2/W structure were carried out by ARXPS using a Surface Science Instruments S-Probe (Al K_α x-ray source). The thickness and the microstructures of various samples were analyzed using both cross-sectional and plan-view transmission electron microscopy (TEM, a Philips CM20 FEG-TEM operating at 200 kV with a point-to-point resolution of 2.4 Å).

Figure 1 shows a cross-sectional high-resolution TEM (HR-TEM) image of ALD-ZrO_2 on ALD-W before the Pt top electrode deposition. The ZrO_2 film had a uniform thickness of 110~115 Å. The deposition rate of ZrO_2 in the ALD system used in this experiment was 0.5~0.6 Å per cycle on an SiO_2 surface, and this matches well with results obtained on the W substrate based on measurement of ZrO_2 thickness using HR-TEM after 200 alternating cycles. Typically, ALD growth based on H_2O and chloride precursors occurs readily on a uniform hydroxyl-terminated surface formed prior to or during the first H_2O pulse. Otherwise, irregular island-type growth is commonly observed at a reduced film growth rate.[7] Therefore, the ALD-W bottom electrode that was covered with a native tungsten oxide during air exposure that may provide a good hydrophilic surface condition for the following ALD-ZrO_2 deposition. This resulted in uniform film growth and the same growth rate obtained as on a SiO_2 surface. As shown in the cross-sectional HR-TEM image, the as-deposited microstructure of the ALD-ZrO_2 film on ALD-W was almost completely polycrystalline, and a tetragonal crystalline ZrO_2 phase was identified through electron diffraction analysis (not presented here). A thin interfacial amorphous layer of thickness of 13~14 Å was observed between the ALD-ZrO_2 and ALD-W, as shown in Fig. 1.

In order to study whether this interfacial layer was native tungsten oxide (WO_x) or compound layer formed by reaction with the overlying ZrO_2, ARXPS was performed. To avoid unwanted interfacial mixing and sputtering artifacts commonly observed during XPS depth profiling of ultrathin high-k dielectrics by ion sputtering,[11] wet chemical etching was incorporated with the ARXPS analysis. The ZrO_2 layer was partially thinned down by exposure to aqueous HF solution ($HF:H_2O=1:10$) until a significant W $4f$ signal coming from the bottom substrate was observed. Sequentially, the take-off angle of generated photoelectrons in relation to the film surface was varied from 35° to 85°, in order to collect depth-profiling information. Figure 2 shows the resulting W $4f$ signals as a function of take-off angle, and signals from both the W substrate and the interfacial layer were observed. Clearly, W $4f$ signals coming from the interfacial layer were located at higher binding energies and the Zr $4p$ signal decreased as the take-off angle increased. To identify the binding status in the interfacial layer, a bare W film with native tungsten oxide was also analyzed using ARXPS. The binding energies of photoelectrons coming from native tungsten oxide were ~37.5 and ~35.5 eV for W ($4f_{7/2}$) and W ($4f_{5/2}$), respectively. These binding energy values agree well with the binding energies from the interface layer shown in Fig. 2. Although it is not clear whether some Zr diffused and mixed with interfacial tungsten oxide during the deposition, the major constituent of the interfacial layer can be identified as tungsten oxide, and not a compound formed by reaction with the adjacent ZrO_2 film. According to the ZrO_2-WO_3 binary phase diagram reported by Chang *et al.*,[12] there is no compound formation and a ZrO_2 solid solution (<5 at. % WO_3) can coexist with WO_3 up to 1100 °C. Our ARXPS data are, therefore, consistent with the reported phase equilibria in this materials system.

Figure 3 shows the $C-V$ characteristics of ALD-W/ZrO_2/Pt capacitors measured at different frequencies. The 18 500 μm^2 circular capacitor was swept from negative to positive bias on top electrode and back to check the amount of hysteresis. Although a modest dispersion was

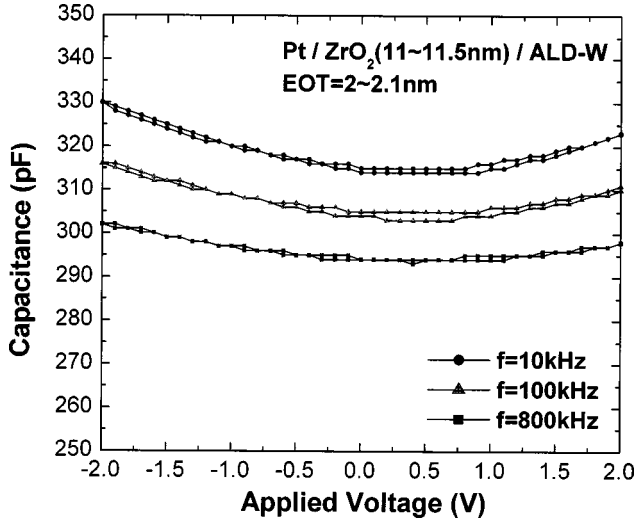

FIG. 3. Capacitance vs applied voltage characteristics of a MIM capacitor structure (Pt/ALD-ZrO_2/ALD-W) for different measurement frequencies. The applied voltage is defined as positive when the top Pt electrode is positively biased.

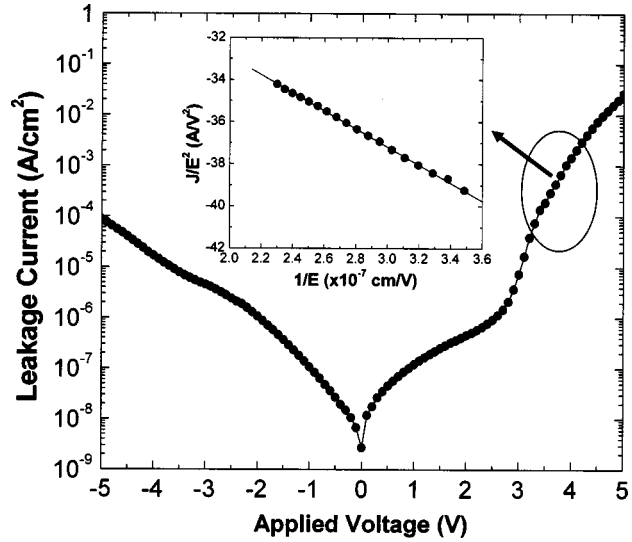

FIG. 4. Leakage current characteristics of a MIM capacitor structure (Pt/ALD-ZrO_2/ALD-W). The inset of the figure shows a J/E^2 vs $1/E$ plot for the positive biasing condition, consistent with Fowler–Nordheim tunneling behavior.

observed with different measuring frequencies and its origin is not clear at this point, the resulting equivalent oxide thickness varied only by ± 1 Å. Based on the measured physical thickness and the capacitance, the apparent equivalent oxide thickness was 20~21 Å and the calculated effective dielectric constant of a capacitor was 22~25, including the interfacial tungsten oxide. Because the reported dielectric constant of a ZrO_2 film on SiO_2/Si is around 25,[5] this measured value is quite reasonable and was not degraded significantly by the presence of the interfacial tungsten oxide. The reported dielectric constant of $WO_{2.9}$ is ~42.[3] A high capacitance per unit area of 16~17 fF/μm^2 was obtained for these ALD-ZrO_2 dielectrics of 110~115 Å thickness, and this is comparable to or even higher than that of typical Ta_2O_5 MIM capacitors. However, because deposition of much thinner ZrO_2 films by ALD is relatively straightforward, there is significant opportunity to scale the areal capacitance to much larger values than those obtained in this work.

Figure 4 shows the leakage current behavior of Pt/ALD-ZrO_2/ALD-W capacitors. Asymmetric $J-V$ characteristics can be seen due to the asymmetric MIM capacitor structure having different Schottky barrier heights at the electrode interfaces. In the case of electron injection from the bottom ALD-W electrode (when the top electrode was positively biased) current-voltage behavior consistent with Fowler–Nordheim tunneling was observed above ~ 3 V in keeping with the J/E^2 versus $1/E$ graph (inset of Fig. 4). Because the interfacial tungsten oxide is relatively thin, we assume that its effect on the barrier height between W and ZrO_2 can be ignored. By assuming an electron effective mass in ZrO_2 as $0.1m_o$,[13] an effective interface potential barrier of ~1.6 eV between ZrO_2 and W was calculated. The leakage current density was around $\sim 10^{-7}$ A/cm^2 at ± 1 V suitable for gigabit DRAM applications.

In summary, ALD growth of ZrO_2 on a W electrode was demonstrated and the resulting Pt-electroded MIM capacitors were characterized. Uniform polycrystalline ZrO_2 in deposited in the ALD growth regime were obtained on the native WO_x surface. Using ARXPS analysis with wet chemical etching, the amorphous interfacial layer between the dielectric and W bottom electrode was identified as WO_x, possibly containing some Zr. Through MIM capacitor fabrication with a Pt top electrode, a 20~21 Å equivalent oxide thickness was obtained and the effective dielectric constant of the capacitor dielectric, including the contribution of the interfacial layer, was 22~25. The leakage current magnitude obtained for carrier injection from the W electrode into the ALD-ZrO_2 dielectric is suitable for application in gigabit DRAM.

This work was supported in part by the NSF/SRC Center for Environmentally Benign Semiconductor Manufacturing, award No. Q423740 and by a Mayfield Stanford Graduate Fellowship. One of the authors would like to thank Dr. C. Knepfler for her useful comments.

[1] *International Roadmap for Semiconductors* (Semiconductor Industry Association, San Jose, CA, 2001); http//public.itrs.net
[2] I.-S. Park, B. T. Lee, S. J. Choi, J. S. Im, S. H. Lee, K. Y. Park, J. W. Lee, Y. W. Hyung, Y. K. Kim, H. S. Park, S. I. Lee, and M. Y. Lee, VLSI Tech. Dig., 42 (2000).
[3] B. C. Lai and J. Y. Lee, J. Electrochem. Soc. **146**, 266 (1999).
[4] C. S. Hwang, S. O. Park, H.-J. Cho, C. S. Kang, H.-K. Kang, S. I. Lee, and M. Y. Lee, Appl. Phys. Lett. **67**, 2819 (1995).
[5] G. D. Wilk, R. M. Wallace, and J. M. Anthony, J. Appl. Phys. **89**, 5243 (2001).
[6] M. Ritala, K. Kukli, P. I. Raisanen, M. Leskela, T. Sajavaara, and J. Keinonen, Science **288**, 319 (2000).
[7] M. Copel, M. Gribelyuk, and E. P. Gusev, Appl. Phys. Lett. **76**, 436 (2000).
[8] S. C. Sun and T. F. Chen, Tech. Dig. - Int. Electron Devices Meet., 687 (1996).
[9] J. H. Huang, Y.-S. Lai, and J. S. Chen, J. Electrochem. Soc. **148**, F133 (2001).
[10] J. W. Klaus, S. J. Ferro, and S. M. George, Thin Solid Films **360**, 145 (2000).
[11] C. M. Perkins, B. B. Triplett, P. C. McIntyre, K. C. Saraswat, S. Haukka, and M. Tuominen, Appl. Phys. Lett. **78**, 2357 (2001).
[12] L. L. Y. Chang, M. G. Scroger, and B. Phillips, J. Am. Ceram. Soc. **50**, 212 (1967).
[13] W. J. Zhu, T. P. Ma, and T. Tamagawa, IEEE Electron Device Lett. **23**, 97 (2002).